THE JOURNAL OF BIOLOGICAL CHEMISTRY
Vol. 276, No. 38, Issue of September 21, pp. 35818–35825, 2001
Printed in U.S.A.
© 2001 by The American Society for Biochemistry and Molecular Biology, Inc.

The Ca^{2+}-binding Proteins S100A8 and S100A9 Are Encoded by Novel Injury-regulated Genes*

Received for publication, May 29, 2001, and in revised form, July 16, 2001
Published, JBC Papers in Press, July 19, 2001, DOI 10.1074/jbc.M104871200

Irmgard S. Thorey‡, Johannes Roth§, Johannes Regenbogen¶, Jörn-Peter Halle¶, Michaela Bittner¶, Thomas Vogl§, Susanne Kaesler‡, Philippe Bugnon‡, Birgit Reitmaier¶, Silke Durka‡, Anja Graf¶, Mandy Wöckner¶, Norman Rieger‖, Alexander Konstantinow, Eckhard Wolf‖, Andreas Goppelt¶, and Sabine Werner‡ ‡‡**

*From the ‡Institute of Cell Biology, ETH Zürich, Hönggerberg, CH-8093 Zürich, Switzerland, §Institute of Experimental Dermatology, University of Münster, Von-Esmarch-Str. 56, D-48129 Münster, ¶SWITCH BIOTECH AG, Fraunhoferstr. 10, D-82152 Martinsried, ‖Institut für Molekulare Tierzucht und Biotechnologie der Ludwig-Maximilians-Universität München, Feodor-Lynen-Str. 25, D-81377 München, and **Klinik für Dermatologie und Allergologie der Technischen Universität München am Biederstein, Biedersteiner Str. 29, D-80802 München Germany*

To gain insight into the molecular mechanisms underlying cutaneous wound repair, we performed a large scale screen to identify novel injury-regulated genes. Here we show a strong up-regulation of the RNA and protein levels of the two Ca^{2+}-binding proteins S100A8 and S100A9 in the hyperthickened epidermis of acute murine and human wounds and of human ulcers. Furthermore, both genes were expressed by inflammatory cells in the wound. The increased expression of S100A8 and S100A9 in wound keratinocytes is most likely related to the activated state of the keratinocytes and not secondary to the inflammation of the skin, since we also found up-regulation of S100A8 and S100A9 in the epidermis of activin-overexpressing mice, which develop a hyperproliferative and abnormally differentiated epidermis in the absence of inflammation. Furthermore, S100A8 and S100A9 expression was found to be associated with partially differentiated keratinocytes *in vitro*. Using confocal microscopy, both proteins were shown to be at least partially associated with the keratin cytoskeleton. In addition, cultured keratinocytes efficiently secreted the S100A8/A9 dimer. These results together with previously published data suggest that S100A8 and S100A9 are novel players in wound repair, where they might be involved in the reorganization of the keratin cytoskeleton in the wounded epidermis, in the chemoattraction of inflammatory cells, and/or in the defense against microorganisms.

After cutaneous injury, a series of biological events takes place that aims at the reconstruction of the damaged skin. Among them are the migration, proliferation, and differentiation of inflammatory, epithelial, and mesenchymal cells. These cells exert specific functions in a temporally and spatially coordinated manner such as the removal of irreversibly destructed tissue, the deposition of new extracellular matrix, and the reestablishment of the cutaneous barrier (1, 2). These processes are well described at the histological level, but little is known about their molecular basis.

To gain insight into the molecular mechanisms that underlie the repair process, we performed a large scale subtractive hybridization screen to systematically identify genes that are differentially expressed in injured compared with normal skin. To minimize the risk of detecting differences in gene expression levels due to changes in cellular composition rather than to transcriptional regulation, we compared normal skin with early (24 h) wounds, because only minor changes in cell type composition occur during the initial wound healing period.

One of the cDNA clones that we obtained encodes the murine S100A8 protein (also known as calgranulin A, MRP8, leukocyte protein L1, or cytokine CP-10). S100 proteins are intracellular Ca^{2+}-binding and Ca^{2+}-modulated proteins that form antiparallel noncovalently linked dimers in solution and play a role in various Ca^{2+}-mediated cellular functions including cell growth and differentiation, energy metabolism, cytoskeletal-membrane interactions; some of the S100 proteins regulate kinase activities or are secreted and perform extracellular functions (3). S100A8 and its dimerization partner, S100A9 (MRP14), are expressed constitutively in neutrophils and monocytes and, after activation, in macrophages and are secreted by these cells, whereas they are absent from normal skin (4–11). However, they are up-regulated in the epidermis as well as in other tissues at sites of inflammation in conditions such as psoriasis, rheumatoid arthritis, inflammatory bowel and lung diseases, and allograft rejection (5, 12–18). Here we demonstrate that S100A8 and S100A9 expression is strongly induced during wound healing. We show that these genes are expressed at high levels in the hyperproliferative wound epithelium during the first week after skin injury as well as in inflammatory neutrophils and macrophages that have infiltrated the wound. Moreover, we detected increased levels of S100A8 and S100A9 in the non-inflamed but hyperproliferative, abnormally differentiated epidermis of activin-overexpressing transgenic mice (19) as well as in activin-overexpressing HaCaT keratinocytes, which differentiate prematurely compared with wild-type cells. We further show that normal and activin-transfected HaCaT cells secrete a substantial fraction of the S100A8/9 proteins they produce into the culture medium. The results presented in this paper indicate that the induction of these genes is not a consequence of the inflammation but rather correlates with an alternative differentiation pathway of the keratinocytes and suggest a novel role for secreted S100A8/9 during wound healing.

* This work was supported by a grant from the Bundesministerium für Bildung und Forschung (BMBF) (to S. W., A. G., and E. W.). The costs of publication of this article were defrayed in part by the payment of page charges. This article must therefore be hereby marked "*advertisement*" in accordance with 18 U.S.C. Section 1734 solely to indicate this fact.

‡‡ To whom correspondence should be addressed: Institute of Cell Biology, HPM D42, ETH Zürich, Hönggerberg, CH-8093 Zürich, Switzerland. Tel.: 0041 1 6333941; Fax: 0041 1 6331174; E-mail: sabine.werner@cell.biol.ethz.ch.

This paper is available on line at http://www.jbc.org

This is an Open Access article under the CC BY license.

EXPERIMENTAL PROCEDURES

Animal Care—BALB/c mice were obtained from Charles River Wiga, Sulzfeld, Germany and from RCC Ltd., Füllinsdorf, Switzerland. They were housed and fed according to German or Swiss Federal guidelines, and all procedures were approved by the local government of Bavaria or of the Kanton Zürich.

Wounding, Preparation of Wound Tissue, and RNA Isolation—Several independent wound healing experiments were performed. For each experiment, 24 BALB/c mice (8–10 weeks of age) were anesthetized with a single intraperitoneal injection of ketamine/xylazine. The hairs on the back of the animals were cut, and the skin was wiped with 70% alcohol. Four full-thickness excisional wounds (5-mm diameter, 8–10 mm apart) were generated on the back of each animal by excising skin and panniculus carnosus. The excised skin pieces were saved and used as unwounded control samples. The wounds were allowed to dry to form a scab. At different time points after injury (1, 3, 5, 7, and 14 days), animals were sacrificed, and the complete wounds including 2 mm of the wound margins were isolated.

For preparation of RNA, the tissue from four animals was combined, immediately frozen in liquid nitrogen, and stored at −80 °C until used for RNA isolation. Total cellular RNA was prepared as described by Chomczynski and Sacchi (20). For *in situ* hybridization, immunohistochemistry, and immunofluorescence, wounds were bisected and fixed for 4 h in 4% paraformaldehyde in phosphate-buffered saline (PBS).[1] Half of each wound was transferred to 15% sucrose in PBS before embedding in tissue-freezing medium (Jung, Köln, Germany) and preparation of frozen sections, and the other half was embedded in paraffin wax and processed according to standard procedures.

Human Biopsies—Biopsies were taken by consent from patients presenting ulcera crura ($n = 4$) of more than 4 months' duration, due to primary or secondary venous insufficiency (size of ulcer >30 cm^2). The biopsies were obtained from the wound edge of chronic wounds and showed no clinical sign of infection. As a control, intact skin from the same patients was taken. For the analysis of physiological wound healing, biopsies were taken from healthy volunteers ($n = 4$), including day-5 wounds (6-mm diameter) and intact skin. After paraformaldehyde fixation, one biopsy was embedded in tissue freezing medium, and the other biopsy (from the same site and the same patient) was embedded in paraffin wax and processed according to standard procedures. All procedures were approved by the local ethics committee of the Technical University of Munich.

cDNA Synthesis, cDNA Subtraction, Reverse Northern Blot, and Screening—Double-stranded cDNA was synthesized starting from 1 μg of total RNA using Superscript II reverse transcriptase (Life Technologies, Inc.) and the SMART PCR cDNA synthesis kit (CLONTECH, Heidelberg, Germany). cDNA subtraction was performed using the PCR-Select cDNA subtraction kit (CLONTECH). cDNA synthesis and subtraction were performed according to the manufacturer's recommendations. 50 ng of subtracted cDNA were cloned directly into 50 ng of the pT-Adv vector (CLONTECH). The ligation mixture was introduced into *Escherichia coli* SURE (Stratagene, Amsterdam, Netherlands) by electroporation (1.7 kV) using an *E. coli* pulser (Bio-Rad). The resulting library was separated into aliquots and frozen in 15% glycerol. An aliquot was plated on selective media containing 100 μM isopropyl-1-thio-β-D-galactopyranoside and 50 μg/ml 5-bromo-4-chloro-3-indolyl β-D-galactopyranoside. A total of 3840 individual recombinant clones were picked and used to inoculate 40 sterile 96-well microtiter plates containing LB medium and ampicillin at 100 μg/ml. After PCR amplification of the cDNA insertions according to the manufacturer's instructions (CLONTECH), the products were dotted in an array onto nylon membranes for duplicate screening using a 384 pin replicator (NUNC, Denmark). The cDNAs were denatured by incubating the prepared membranes on polyethylene-coated Whatman paper soaked in 0.4 M NaOH for 20 min followed by washing the membranes with Tris EDTA buffer. Fixation was performed by baking (30 min at 80 °C) followed by UV-cross-linking (256 nm, 120 mJ/cm^2). The filters were hybridized under stringent conditions (25 mM sodium phosphate buffer pH 7.5, 125 mM NaCl, 7% SDS at 67 °C) with equivalent amounts of ^{32}P-labeled subtracted double-stranded cDNAs of equal specific activity derived from the wound minus skin and the skin minus wound subtractions. Filters were washed under stringent conditions (hybridization buffer diluted 1:10 at 67 °C) and analyzed using the PhosphorImager (Storm 860, Molecular Dynamics, Krefeld, Germany). Differentially expressed cDNAs were identified by comparison of the resulting signals.

RNase Protection Assay—RNase protection assays were performed according to (21). 276- and 267-base pair fragments corresponding to the full-length coding sequence of S100A8 and nucleotides 108–375 of the coding sequence of S100A9 served as templates for the generation of ^{32}P-labeled antisense riboprobes. The template for the human activin βA probe was recently described (19).

Radioactive in Situ Hybridization—Frozen sections (6 μm) from the middle of 5-day-old wounds were hybridized as described (22). 246- and 267-base pair fragments corresponding to nucleotides 97–343 of the coding and 3′-untranslated sequence of S100A8 and nucleotides 108–375 of the coding sequence of S100A9 served as templates for the generation of ^{35}S-labeled antisense riboprobes. After hybridization, sections were coated with Kodak NBT2 nuclear emulsion (Integra Bioscience AG, Wallisellen, Switzerland) and exposed in the dark for 3 weeks. After development, sections were counterstained with Mayer's hemalum and eosin, mounted, and analyzed using a Zeiss Axiophot microscope equipped with a Jenoptik ProgRes 3008 CCD camera.

Non-radioactive in Situ Hybridization—Partial cDNA fragments of human S100A8 (nucleotides 72–241) and human S100A9 (nucleotides 13–375) were amplified under standard PCR conditions. The primers used were as follows: 5′-AATTAACCCTCACTAAAGGGG GAA TTT CCA TGC CGT CTA CAG G-3′ (S100A8 sense primer, with T3 promoter sequence underlined); 5′-TAATACGACTCACTATAGGGC CCA CGC CCA TCT TTA TCA CCA G-3′ (S100A8 antisense-primer, with T7 promoter sequence underlined); 5′-AATTAACCCTCACTAAAGGGG GTG GCT CCT CGG CTT TGA CA-3′ (S100A9 sense primer, with T3 promoter sequence underlined); 5′-ATTTAGGTGACACTATAGAATAC CCC GAG GCC TGG CTT ATG GT-3′ (S100A9 antisense primer, with Sp6 promoter sequence underlined). Human cDNA of 5-day-old wounds was subjected to 40 cycles of PCR (94 °C for 30 s, 55 °C for 30 s, and 72 °C for 1 min 30 s). Resultant PCR products were subcloned into the vector pCR 2.1 TOPO (Invitrogen, Leek, Netherlands) and verified by sequencing. Digoxigenin-labeled sense and antisense riboprobes were synthesized with T3, T7, or Sp6 polymerase using the digoxigenin RNA labeling mix from Roche Molecular Biochemicals according to the manufacturer's protocol. Non-radioactive *in situ* hybridization was performed as previously described (23). Briefly, deparaffinized sections were treated with proteinase K and acetylated. For prehybridization, the sections were overlaid with hybridization mix (50% formamide, 4× SSC (1× SSC = 0.15 M NaCl and 0.015 M sodium citrate), 5% dextran sulfate, 1× Denhardt's solution, 250 μg/ml tRNA, 500 μg/ml salmon sperm DNA) for at least 1 h at 55 °C. Hybridization was performed overnight at 55 °C with 80 ng of sense or antisense probe (diluted in hybridization mix) per section. After stringent washing steps (2× SSC for 30 min at room temperature, 50% formamide, 2× SSC for 30 min at room temperature, 50% formamide, 2× SSC for 30 min at 50 °C, 1× SSC for 15 min at room temperature) and RNase A digestion, the hybridized digoxigenin-labeled probes were detected by alkaline phosphatase-conjugated anti-digoxigenin antibody (DAKO, Hamburg, Germany). Hybridization signals were visualized using 5-bromo-4-chloro-3-indolyl phosphate and nitro blue tetrazolium. Some sections were counterstained with Nuclear Fast Red (Vector Laboratories, Peterborough, England).

Immunohistochemical Staining—Sections were processed for immunoperoxidase staining as described previously (17). Briefly, acetone-fixed sections (5 μm) were placed in PBS containing 0.1% hydrogen peroxide (v/v) and 0.12 M sodium azide (Merck) to inhibit endogenous peroxidase activity. After blocking nonspecific protein binding with 1% (w/v) bovine serum albumin (Sigma) in PBS, sections were incubated with 1 μg/ml antibodies against S100A8 or S100A9 (24, 25) or with the monoclonal antibody 27E10, which exclusively detects the S100A8/A9 heterodimer but not single monomers (27), followed by peroxidase-conjugated secondary antibodies (Dianova). Peroxidase activity was detected with 3-amino-9-ethylcarbazole (Sigma). Sections were counterstained with Mayer's hemalum (Merck). For negative controls, specific antibodies were replaced by isotype-matched antibodies of irrelevant specificity.

Immunofluorescence—Paraffin was removed from sections that had been prepared from the middle of 5-day-old wounds and tail skin of activin-overexpressing and wild-type mice. After rehydration, sections were allowed to dry. HaCaT cells were grown to confluence on positively charged microscope slides (Superfrost; Menzel Gläser, Germany), and some specimens were incubated with 10 μM Ca^{2+} ionophore A23187 (Calbiochem) for 1 h to ensure the activation of Ca^{2+}-dependent cellular processes before fixation with 4% paraformaldehyde in PBS for 10 min, washing with PBS, and postfixation with ice-cold acetone for 10 min. Specimens were then incubated overnight at 4 °C with specific antisera to S100A8 or S100A9 (24, 25) and, in some instances, with a mouse

[1] The abbreviations used are: PBS, phosphate-buffered saline; PCR, polymerase chain reaction; m-, murine; h-, human.

monoclonal antibody directed against human cytokeratin 10 (DAKO), diluted in PBS containing 12% bovine serum albumin. After washing with PBS, sections were incubated for 1 h at room temperature with fluorescein isothiocyanate-conjugated secondary antibody directed against rabbit and/or mouse immunoglobulins (Roche Molecular Biochemicals). After washing with PBS, sections were allowed to dry and mounted with Mowiol (Hoechst, Frankfurt, Germany) or *n*-propyl gallate/Tris/glycerol, and fluorescence was analyzed either by using a Zeiss Axioplan microscope equipped with a Hamamatsu three-color CCD camera or by using a Leica DM IRBE fluorescence microscope equipped with a TCSNT confocal laser system.

SDS-Polyacrylamide Gel Electrophoresis and Western Blot—Tissues were homogenized in Tris buffer containing 8 M urea, protein concentration was determined by the BCA method, and 30-μg aliquots were boiled in sample buffer containing 100 mM dithiothreitol before SDS-polyacrylamide gel electrophoresis and blotting onto nitrocellulose membrane (Protran, Schleicher &Schuell). Membranes were then incubated overnight at 4 °C with specific antisera to S100A8 or S100A9 (24, 25) followed by alkaline phosphate-conjugated anti-rabbit IgG (Promega, Heidelberg, Germany). Antibody binding was visualized using nitro blue tetrazolium and 5-bromo-4-chloro-3-indolyl phosphate (Promega).

Cell Culture and Quantitative Enzyme-linked Immunosorbent Assay of S100 Proteins—Vector-transfected and activin βA-transfected HaCaT cells were grown in 100-mm tissue culture dishes in 10 ml of Dulbecco's modified Eagle's medium (Sigma) supplemented with 10% fetal calf serum (Amimed; Bioconcept, Allschwil, Switzerland) and 200 mg/liter Geneticin (Life Technologies, Inc.). For determination of secreted S100A8/9, the medium was replaced by serum-free DMEM at confluence, and aliquots of 300 μl of supernatant were sampled from the dishes immediately and at different time points thereafter. Cells were pelleted from the supernatant, and the supernatant was snap-frozen in liquid nitrogen. In one experiment, the number of dead cells floating in the supernatant was analyzed using trypan blue exclusion and found to be not greater than 0.5% of the total number of cells. At the end of the experiment, the cells on each plate were trypsinized and counted for normalization to cell number. For determination of intracellular S100A8/9, cells were trypsinized at confluence, and an aliquot was counted using a hemocytometer. Cells were then pelleted and snap-frozen in liquid nitrogen. A quantitative sandwich enzyme-linked immunosorbent assay for S100A9 was performed as described previously (26).

RESULTS

S100A8 and S100A9 Expression Is Strongly Up-regulated after Wounding—Using the PCR-Select kit we constructed a subtractive cDNA library of normal *versus* wounded murine skin and vice versa in order to identify genes that are either up- or down-regulated after skin injury. One of the ESTs we obtained from the screen for up-regulated genes corresponded to the full-length murine S100A8 (mS100A8) cDNA. To confirm the differential expression, we analyzed the mS100A8 mRNA levels during the different stages of wound repair by RNase protection assay. As shown in Fig. 1*A*, mS100A8 mRNA expression, which was barely detectable in healthy skin, was dramatically up-regulated during the first week after injury and subsequently decreased until it had reached low levels by the end of the second week after wounding, when the wounds were fully healed. Identical results were obtained with probes that were either transcribed from the initial EST or from the full-length sequence (shown is the result obtained with the full-length probe). Moreover, this result was confirmed by analysis of independently prepared RNAs using real time reverse transcriptase-PCR. By this technique, a 40-fold increase in mS100A8 mRNA levels in 1-day wounds compared with intact skin was measured (data not shown).

Because S100A8 is usually co-expressed with its dimerization partner, S100A9, we determined whether mS100A9 mRNA is also up-regulated after injury. Indeed, as shown in Fig. 1*B*, mS100A9 expression was strongly induced in 1–7-day-old wounds. Moreover, mS100A8 and mS100A9 mRNA levels seemed to be regulated in a strictly coordinated fashion. This result was reproduced twice with different sets of RNAs from independent wounding experiments. To determine the expression levels of mS100A8 and mS100A9 proteins within the wounds, Western blot analysis was performed with specific antisera and an alkaline phosphatase-conjugated secondary antibody. As described previously, the specificity of these antisera has been verified by Western blot analysis of lysates prepared from monocytes and granulocytes as well as by immunoreactivity against recombinant S100A8 and S100A9 and against S100A8 and/or S100A9 transfected fibroblastic cell lines (24, 25). Western blot analysis of wound lysates revealed that mS100A8 and mS100A9 proteins were also induced after injury, with kinetics that correlated with those of the mRNAs (Fig. 1, *D* and *E*).

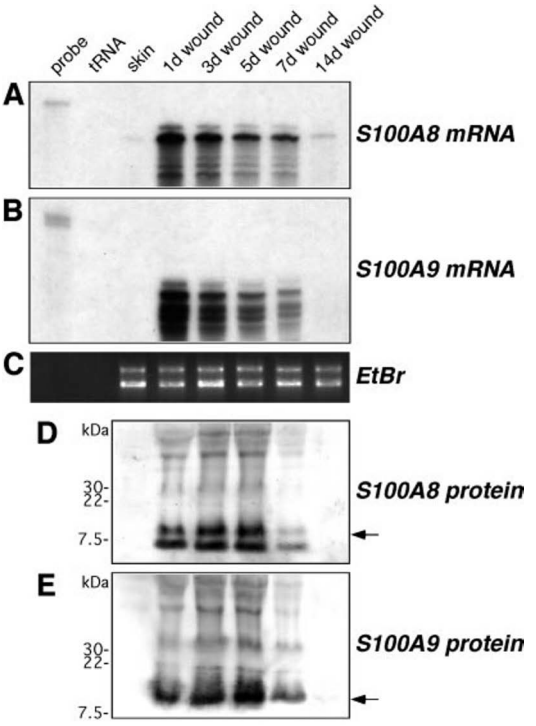

FIG. 1. **Expression of S100A8 and S100A9 mRNA and protein is strongly induced during wound healing.** Aliquots of 20 μg from batches of total RNA that was prepared from murine skin wounds at different times after injury were subjected to RNase protection analysis with antisense probes to the full-length coding sequences for mS100A8 (*panel A*) or mS100A9 (*panel B*), or 1-μg aliquots were separated on an agarose gel and stained with ethidium bromide (*EtBr; panel C*). *probe*, 1000 cpm of the radioactive probes were used as a standard for size and intensity of signal; *tRNA*, 20 μg of tRNA was used as a negative control. The film was exposed overnight without the aid of an intensifier screen. Aliquots of 30 μg from batches of total protein lysate that was prepared from murine skin wounds at different times after injury were subjected to SDS-polyacrylamide gel electrophoresis and Western blotting with specific antisera to mS100A8 (*panel D*) and mS100A9 (*panel E*). Binding of the alkaline phosphate-conjugated secondary antibody was visualized by nitro blue tetrazolium and bromo-chloro-indolyl phosphate. Sizes of marker proteins are indicated on the left of the panels. The bands corresponding to the mS100A8 and mS100A9 monomers are indicated by *arrows*. A double band for S100A8 is frequently observed and most likely results from partial proteolytic cleavage during tissue preparation. *d*, day.

The Hyperproliferative Wound Epithelium Is a Novel Site of S100A8 and S100A9 Expression—To identify and localize the mS100A8/A9-expressing cell types within the wound, we performed *in situ* hybridization on sections of 5-day-old wounds. At this stage after injury, a thick hyperproliferative epithelium as well as extensive granulation tissue containing various inflammatory cells is present in the wound. As shown in Fig. 2, ^{35}S-labeled antisense probes for mS100A8 (Fig. 2, *A* and *B*) and mS100A9 (Fig. 2, *C* and *D*) yielded striking hybridization sig-

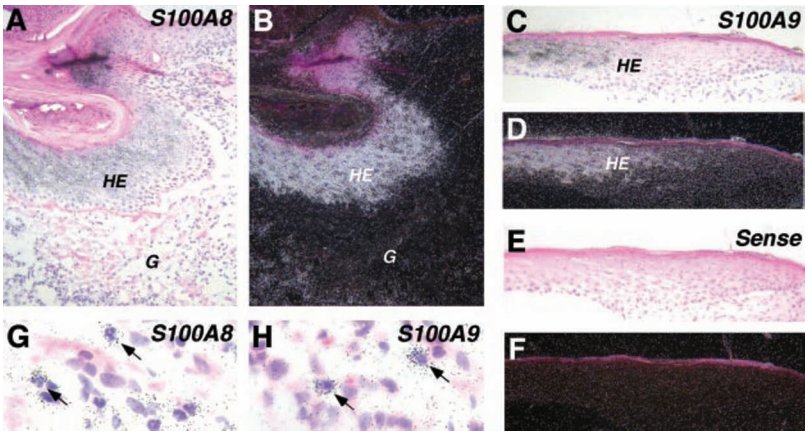

FIG. 2. **S100A8 and S100A9 mRNAs are localized to differentiating keratinocytes of the hyperproliferative wound epithelium.** 6-μm frozen sections of 5-day wounds were hybridized to ^{35}S-labeled antisense probes, which recognized coding sequences of mS100A8 (*panels A*, *B*, and *G*), mS100A9 (*panels C*, *D*, and *H*), or to a mS100A9 probe transcribed in the sense direction (*panels E* and *F*). Sections were exposed for 3 weeks, counterstained with Mayer's hemalum and eosin, and viewed at magnifications of 200× (*panels A–F*; shown is the area of the epithelial edge to the right of the center of the wound) or 630× (*panels G* and *H*). Specific hybridization is indicated by dark grains in the bright field views (*panels A*, *C*, *E*, *G*, and *H*) and by bright grains in the dark field views (*panels B*, *D*, *F*). *G*, granulation tissue; *HE*, hyperproliferative epithelium; *arrows* in *panels G* and *H*, mS100A8 and mS100A9 expressing inflammatory neutrophils that can be identified by their characteristic segmented nuclei.

nals throughout the suprabasal layers of the hyperproliferative epithelium (Fig. 2, *A–D*), indicating that differentiating wound keratinocytes express high levels of mS100A8 and mS100A9 mRNAs. By contrast, keratinocytes at a distance from the wound did not express these genes (data not shown). Inspection of the granulation tissue at high magnification also revealed a specific population of cells that were decorated with silver grains (Fig. 2, *G* and *H*). The shape of their nuclei suggests that these cells are neutrophils and macrophages, which are known producers of S100A8 and S100A9 (4–11). No signals were obtained with probes transcribed in the sense direction (Fig. 2, *E* and *F*, for mS100A9; data not shown for mS100A8).

Subsequently, we performed immunohistochemical stains and immunofluorescence analysis with specific antisera to localize the mS100A8 and mS100A9 proteins. Fig. 3, *A-C*, shows overviews of sections through 5-day-old wounds that were immunostained using a peroxidase-conjugated secondary antibody. In sections stained for mS100A8 (Fig. 3*A*) and S100A9 (Fig. 3*B*), the reaction product was seen within the hyperthickened wound epidermis (*arrows* in Fig. 3, *A* and *B*) as well as in punctate locations throughout the deeper layers of the dermis and the granulation tissue, whereas control sections stained with preimmune sera did not show this specific stain (Fig. 3*C*). To localize both mS100A8 and mS100A9 in the hyperproliferative epidermis at the wound edge at higher resolution, we performed indirect immunofluorescence on serial sections of several 5-day-old wounds. A typical result is shown in Fig. 3, *D–F*. Immunofluorescent label decorated the cytoplasm of the suprabasal differentiating wound keratinocytes in the sections that were stained for mS100A8 (Fig. 3*D*) and mS100A9 (Fig. 3*E*), whereas no epidermal stain was seen when the first antibody was omitted (Fig. 3*F*). Furthermore, by staining sections of earlier and later wounds, we determined that in 3-day-old wounds, the suprabasal cells of the emerging hyperproliferative epithelium already were highly immunopositive for mS100A8 and mS100A9, whereas at day 13 after injury, when the epidermis reversed to a non-hyperproliferative state, no immunoreactivity was seen in keratinocytes (data not shown).

S100A8 and S100A9 Are Induced in Acute and Chronic Human Wounds—To determine whether the up-regulation of S100A8 and S100A9 also occurs in injured human skin, we prepared digoxigenin-labeled antisense probes for the human homologs, hS100A8 and hS100A9, and hybridized them to sections of human wounds. As seen in Fig. 4, both mRNAs were strongly

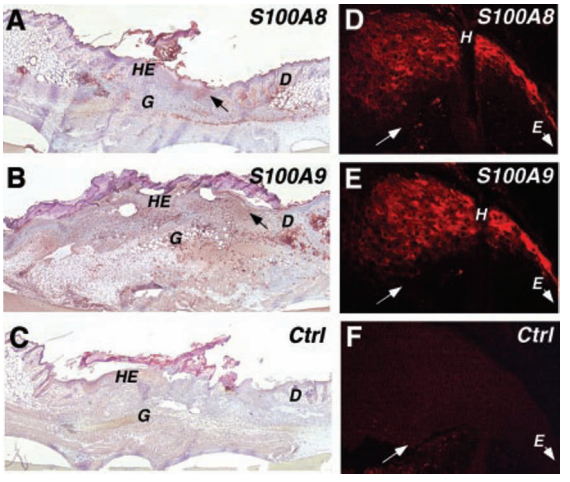

FIG. 3. **Localization of S100A8 and S100A9 proteins in sections of murine wounds.** 7-μm paraffin sections of 5-day-old murine wounds were stained by the indirect peroxidase method using specific polyclonal antisera directed against mS100A8 (*panel A*), mS100A9 (*panel B*), or using pre-immune sera (*panel C*). Specific reaction product appears in *red*. Sections were counterstained with Mayer's hemalum and viewed at magnifications of 25×. *D*, dermis; *HE*, hyperproliferative epithelium; *G*, granulation tissue; *arrows* in *panels A* and *B*, immunopositive hyperproliferative epithelium. Serial paraffin sections of 5-day-old murine wounds were stained with specific polyclonal antisera directed against mS100A8 (*panel D*) or mS100A9 (*panel E*), followed by Cy3-conjugated anti-rabbit-IgG. In *panel F*, the specific first antibody was omitted. Shown is a view of the hyperproliferative epithelial tongue at the wound edge at 250× magnification. *H*, position of a hair shaft; *E with an arrow*, direction toward normal epidermis; *arrows*, position of the basal keratinocyte layer. *Ctrl*, control.

expressed in suprabasal epithelial cells of acute full-thickness excisional skin wounds that were taken from healthy adult volunteers (n = 4) 5 days after injury (Fig. 4, *C–F*). Moreover, in sections prepared from chronic venous ulcers (n = 3 for S100A8 and n = 1 for S100A9), we observed a strong hybridization signal in the suprabasal layers of the strongly thickened epithelium around the edge of these chronic wounds (Fig. 4, *G* and *H*). Intact human skin was devoid of hybridization signal (Fig. 4, *A* and *B*), as were sections that had been hybridized to probes transcribed in the sense direction (data not shown). In confirmation of previous data (13, 15, 16, 18, 28), we also found hS100A8 and hS100A9 expression in lesional but not in the non-affected skin of

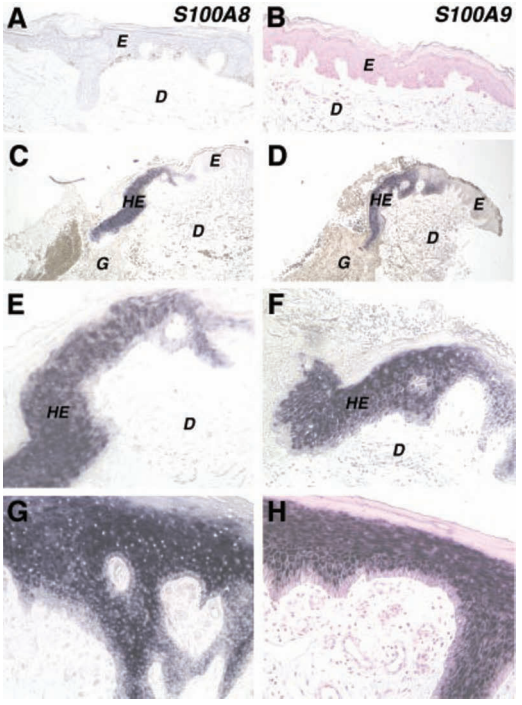

FIG. 4. **S100A8 and S100A9 mRNAs are up-regulated in acute and chronic human wounds.** Paraffin sections of intact human skin (*panels A* and *B*), acute human wounds at day 5 after injury (*panels C–F*), or chronic *wounds (panels G* and *H;* Ulcus cruris lateralis) were hybridized to digoxigenin-labeled antisense probes for hS100A8 (*panels A*, *C*, *E*, and *G*) or hS100A9 (*panels B*, *D*, *F*, and *H*) mRNAs. Reaction product appears in a *grayish-purple color*. Sections were viewed at magnifications of 25× (*panels A–D*) and 100× (*panels E–H*). *E*, epidermis; *D*, dermis; *G*, granulation tissue; *HE*, hyperproliferative epithelium. Note that some sections (*panels B* and *H*) were counterstained with nuclear fast red.

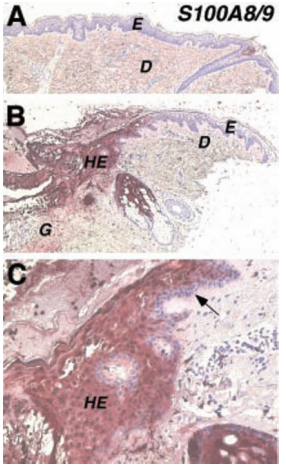

FIG. 5. **The heterodimeric S100A8/9 complex is present in the hyperproliferative epidermis of human wounds.** Paraffin sections of intact human skin (*panel A*) or acute human wounds at day 5 after injury (*panels B* and *C*) were stained with a specific monoclonal antibody directed against the hS100A8/9 heterodimer. The reaction product appears in *red*. Sections were counterstained with Mayer's hemalum and viewed at magnifications of 25× (*panels A* and *B*) or 100× (*panel C*). *E*, epidermis; *D*, dermis; *G*, granulation tissue; *HE*, hyperproliferative epithelium. *Arrow* in *panel C*, basal epithelial layer, exhibiting very little immunoreactivity.

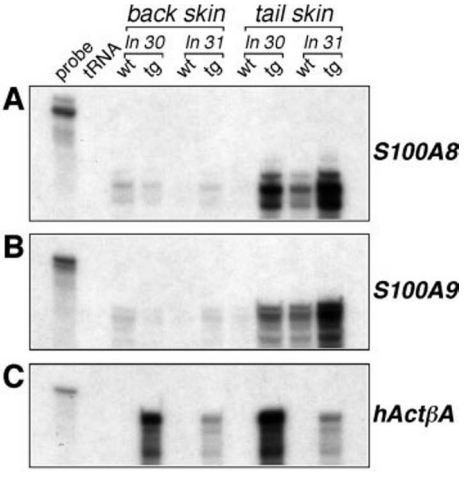

FIG. 6. **Increased S100A8 and S100A9 mRNA expression in the tail skin of activin-overexpressing transgenic mice.** Aliquots of 20 μg from batches of total RNA that was prepared from tail or back skin of two lines (*ln 30* or *ln 31*) of transgenic mice (*tg*) that overexpress the activin βA chain in the epidermis or of their wild-type siblings (*wt*) were subjected to RNase protection analysis with antisense probes to the full-length coding sequences for mS100A8 (*panel A*) or mS100A9 (*panel B*) or with a probe to the human activin βA chain (*panel C*). *probe*, 1000 cpm of the radioactive probes were used as a standard for size and intensity of signal; *tRNA*, 20 μg of tRNA was used as a negative control. The film was exposed for 2 days (*panels A* and *B*) or overnight (*panel C*) without the aid of an intensifier screen.

psoriatic patients (data not shown).

To determine whether hS100A8 and hS100A9 proteins are present in the heterodimeric form in human wounds, we prepared immunohistochemical stains using the monoclonal antibody 27E10, which specifically recognizes the human S100A8/A9 heterodimer (27), and a peroxidase-conjugated secondary antibody. As shown in Fig. 5, the reaction product decorated the suprabasal hyperproliferative keratinocytes of a 5-day-old wound (Fig. 5, *B* and *C*), whereas the basal keratinocytes were largely devoid of stain (Fig. 5*C*, *arrow*). No antibody stain was detected in intact skin (Fig. 5*A*). This result shows that hS100A8 and hS100A9 proteins are present in the suprabasal keratinocyte layers of wounded skin, and moreover, they are assembled into the heterodimeric complex.

S100A8 and S100A9 Are Up-regulated in the Hyperthickened Epithelium of Activin-overexpressing Transgenic Mice—To determine whether the up-regulation of S100A8 and S100A9 in keratinocytes is related to inflammation or to the hyperproliferative activated state of the epithelium, we analyzed the expression of the two genes in the skin of transgenic mice that overexpress the human transforming growth factor β superfamily member activin A in the basal layer of the epidermis. In the tail skin and to a much lesser extent also in the back skin of these mice, a hyperthickened epithelium develops without obvious signs of inflammation. This epithelium is also characterized by abnormal keratinocyte differentiation (19). In the RNase protection assay shown in Fig. 6, mRNAs from two lines of transgenic mice (*lines 30* and *31*) expressing high levels of recombinant activin (Fig. 6*C*) were compared with their wild-type siblings. In both transgenic lines, mRNA levels for mS100A8 (Fig. 6*A*) and mS100A9 (Fig. 6*B*) were found to be strongly increased in transgenic compared with wild-type tail skin, whereas expression levels in the back skin of both transgenic and wild-type mice were always lower (Fig. 6, *A* and *B*) and slightly variable between individual mice (data not shown). No interleukin 1β transcripts were detected by RNase protection analysis of the same batches of tail and back skin RNAs (data not shown). Furthermore, tumor necrosis factor-α was not expressed in the skin of these mice,[2] and no inflammatory infiltrate was seen. These findings strongly suggest that up-regulation of S100A8 and S100A9 occurs in the absence of inflammation.

[2] S. Werner, unpublished data.

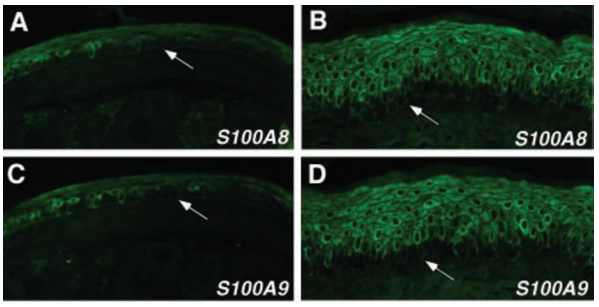

FIG. 7. **S100A8 and S100A9 proteins are co-expressed within the hyperthickened tail epithelium of activin-overexpressing mice.** Serial paraffin sections prepared from the tail skin of activin-overexpressing transgenic mice or their wild-type siblings were stained with specific polyclonal antisera directed against mS100A8 (*panels A* and *B*) or mS100A9 (*panels C* and *D*) followed by fluorescein-conjugated anti-rabbit-IgG. Shown are a view of an area of wild-type epidermis that contained a few immunopositive cells (*panels A* and *C*) and a view of a patch of transgenic epidermis containing several layers of highly immunoreactive suprabasal cells (*panels B* and *D*). The *arrows* in *panels A-D*, position of the basement membrane separating epidermis and dermis. Sections were viewed at 250× magnification.

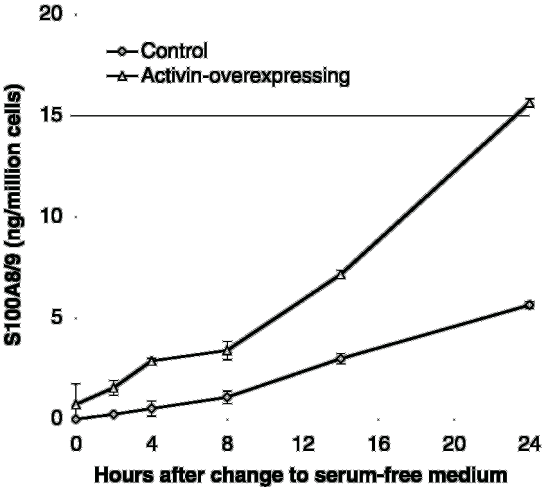

FIG. 8. **S100A8/9 is secreted by vector-transfected and activin-overexpressing HaCaT human keratinocytes.** Aliquots of cell culture supernatant were taken from duplicate confluent plates of activin-overexpressing cells and cells transfected with a vector containing only the neomycin resistance gene (*Control*) at different time points after switching to serum-free medium. The content of S100A8/9 was measured by a sandwich enzyme-linked immunosorbent assay for S100A9 (26). The absolute values were determined by interpolating a standard curve prepared with defined concentrations of purified human complex of S100A8/A9. Numbers were normalized to 10^6 cells and plotted against time.

To localize mS100A8 and mS100A9 expression in the tail skin, we performed immunofluorescence with serial sections prepared from several transgenic and wild-type mice (Fig. 7). Most sections of wild-type animals stained for mS100A8 and mS100A9 did not contain any labeled epithelial cells. A few patches of immunopositive cells were detected in the normal epidermis of one out of five mice only (Fig. 7, *A* and *C*). In transgenic mice, on the other hand, both proteins were co-expressed at high levels by epithelial cells residing within the suprabasal layers of the strongly hyperthickened epidermis (Fig. 7, *B* and *D*), although the expression pattern was patchy. No increased numbers of immunopositive inflammatory cells were detected in sections taken from transgenic mice, compared with wild-type mice (Fig. 7, *A–D*, and data not shown). Sections that had not received specific first antibody were devoid of stain (data not shown). These results demonstrate that up-regulation of mS100A8 and mS100A9 can occur in a hyperproliferative epidermis in the absence of inflammation.

S100A8 and S100A9 Are Expressed and Secreted by a Differentiated Subpopulation of HaCaT Keratinocytes—To answer the question of whether the S100A8/9 dimer is secreted by keratinocytes that express it, we used HaCaT human keratinocyte cell lines, which were transfected either with an activin βA expression construct, resulting in premature initiation of differentiation in many of these cells (19), or with a vector containing only the neomycin resistance gene. For the detection of the S100A8/S100A9 heterodimer we used a quantitative sandwich enzyme-linked immunosorbent assay for S100A9, since the latter only forms heterodimers with S100A8 but no homodimers. We first determined that HaCaT cells contain intracellular hS100A8/9 heterodimers and, furthermore, that activin-overexpressing cells contain significantly higher levels (37.98 + 2.86 ng/10^6 cells) than neo-transfected control cells (15.5 + 11.6 ng/10^6 cells; the determination was performed twice with cells of slightly different passage number). Next, we analyzed the kinetics of hS100A8/9 secretion into serum-free culture medium. Fig. 8 shows that under these conditions hS100A8/9 is secreted at substantial levels by the HaCaT cells, as the amount accumulating within 24 h in the culture medium corresponds to 35–40% of the intracellular content of an equal number of cells at the beginning of the experiment. Furthermore, the secretion level of activin-overexpressing HaCaT cells was significantly higher than that of wild-type cells (by a factor of 1.5–2.5; the experiment was repeated three times with cells of slightly different passage number, and duplicate plates were prepared for each experiment). By trypan blue staining of the cells floating in the culture supernatant, we verified that the contribution of S100A8/9 proteins released into the culture medium by lysed dead cells was negligible, since less than 0.5% of the total number of cells were dead.

To determine whether every HaCaT cell or only a subpopulation of differentiated cells express S100A8 and S100A9, we performed double immunofluorescence with antibodies directed against hS100A8 or hS100A9 and human cytokeratin 10 (hK10), a marker of early keratinocyte differentiation. Fig. 9, *A–C* and *D–F*, show corresponding areas of cultures of activin-overexpressing cells stained with hS100A8 (Fig. 9*A*) or hS100A9 (Fig. 9*D*) and hK10 antibodies (Fig. 9, *C* and *F*) and imaged by confocal laser scanning microscopy. As can be seen in the overlays of both signals (*yellow color* in Fig. 9, *B* and *E*), most but not all cells that express either protein also express the other, indicating that, similar to the *in vivo* situation, hS100A8 and hS100A9 expression in HaCaT cells is associated with the differentiated state. A similar result was also obtained with vector-transfected keratinocytes, although the percentages of K10-, S100A8-, and S100A9-positive cells were lower (data not shown). The subcellular localization of the hS100A8 and hS100A9 proteins in comparison to hK10 was determined by scanning individual optical sections of immunopositive cells at a high magnification (shown for activin-transfected cells in Fig. 9, *G–I* and *K–M*). Signals from hS100A8 (Fig. 9*G*) and hS100A9 (Fig. 9*K*) immunostainings revealed that both proteins were distributed throughout the cells. However, toward the cell periphery a mesh-like pattern of higher and lower hS100A8/9 protein concentrations was observed. In some peripheral areas of each cell (*arrows* in Fig. 9, *G–M*), regions of high S100A8/9 concentration co-localized with the K10 signal (Fig. 9, *I* and *M*). This co-localization was also seen in vector-transfected cells and was observed irrespective of treatment with the Ca^{2+} ionophore A23187 before fixation, presumably because within the immunopositive differentiated cells, Ca^{2+}-dependent cellular processes were already activated. These results suggest an association of some of the S100A8/9 proteins with parts of the keratin filament network.

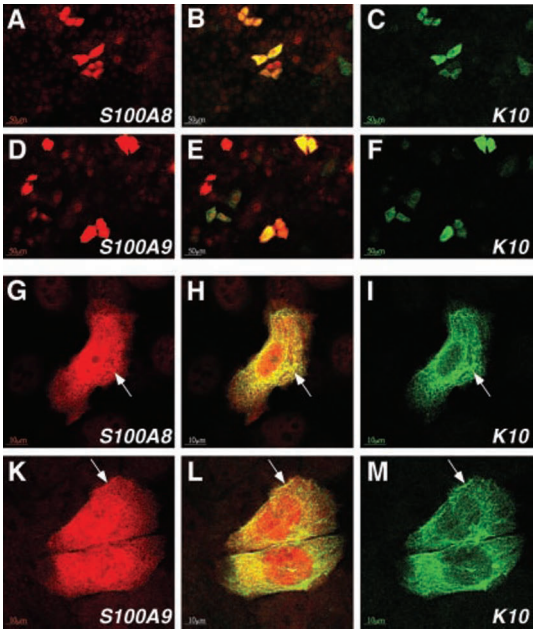

FIG. 9. **Coexpression of S100A8 and S100A9 with the differentiation marker cytokeratin 10 in HaCaT keratinocytes.** Activin-overexpressing HaCaT cells were stained with specific polyclonal antisera directed against hS100A8 (*panels A* and *G*) or hS100A9 (*panels D* and *K*) and with a monoclonal antibody to human cytokeratin 10 (*panels C*, *F*, *I*, *M*) followed by Cy3-conjugated anti-rabbit-IgG and fluorescein-conjugated anti-mouse-IgG. Cells were viewed by confocal laser microscopy. To detect co-localization, an overlay was prepared of the images from the *red* and *green* channels (*panels B*, *E*, *H*, *L*). *Arrows* in *panels G–M*, areas where high level hS100A8 or hS100A9 expression and cytokeratin filaments are co-localized. Cells were scanned at 250× (*panels A–F*) or 630× (*panels G–M*) magnification.

DISCUSSION

To gain insight into the molecular mechanisms that underlie the wound-healing process, we initiated a large scale screen for wound-regulated genes. This strategy was chosen since a series of previous studies from our laboratory had revealed important functional roles of genes that are differentially expressed between wounded and unwounded skin. These genes encode cytokines, growth factors, and their receptors, which play a role in the signaling network that orchestrates skin reconstruction in a temporally and spatially coordinated manner (21, 29–34), proteins with a protective function, *e.g.* proteins that limit the amount of inflammation or oxidative stress or control bacterial infection (35–37), or extracellular matrix molecules, which erect a scaffold into which cells can grow and that can bind growth factors and other essential molecules (38).

In our initial screen, we identified mS100A8 as a gene that was strongly up-regulated after injury and, subsequently, we identified its dimerization partner, mS100A9, which was up-regulated in a coordinated fashion. S100A8 and S100A9 have been previously characterized as Ca^{2+}-binding proteins whose expression is linked to inflammatory processes in myeloid cells and in diseased epidermis, which is characterized by abnormal differentiation (5, 12–17, 28, 39, 40). Here we report the injury-regulated induction of the genes for these two Ca^{2+}-binding proteins, not only in the inflammatory leukocytes recruited into the wound but also in differentiating suprabasal wound keratinocytes which express them at high levels during the hyperproliferative phase. We further show that human HaCaT keratinocytes express these proteins in cell culture and secrete them at high levels into the culture medium.

S100A8 and the S100A8/9 heterodimer are also secreted by other epithelial cells and by activated monocytes (41, 42), and there are at least two potential extracellular functions of these proteins that may be of physiological relevance in the context of wound healing. First, the heterodimer has been shown to display striking antimicrobial properties, as it is inhibitory and even toxic toward various strains of pathogenic microorganisms (43–45). Thus, one possible reason for the up-regulation of the two dimerization partners could be control of microbial infection at the wound site.

Second, murine S100A8 was identified as a potent chemotactic molecule that has the capacity to recruit myeloid cells *in vitro* and *in vivo* (46). The moiety performing this function is a non-covalent homodimer of two S100A8 molecules, which is the favored form in low Ca^{2+} concentrations (3). It was further shown that the non-covalent homodimer is oxidized to a non-functional disulfide-linked homodimer by the action of hypochlorite under conditions similar to those prevailing during inflammatory processes. This process may limit leukocyte recruitment to the site of inflammation on one hand and protect cells from excessive oxidative damage by neutralizing reactive oxygen species on the other hand (3). Thus, if the murine S100A8 protein is secreted by some of the cells expressing it within the wound, it may play a role in the regulatory network that controls the inflammatory process. A function of S100A8 in the control of inflammation in the mouse is also suggested by its targeted inactivation phenotype; null embryos are infiltrated with maternal inflammatory cells and resorbed at embryonic day 9.5, whereas in embryos with a functional allele, fetal cells, which infiltrate the deciduum before embryonic day 9.5, express mS100A8 and through this are thought to prevent resorption (47). However, some functional differences may exist between murine and human S100A8. The human protein was neither shown to be chemotactically active nor to form homodimers (3, 46, 48). Thus, the physiological relevance of these extracellular effects during the process of wound healing is still not clear.

Evidence from activin-overexpressing mice, which do not show inflammation in non-wounded skin (19), suggests that expression of S100A8 and S100A9 by the suprabasal keratinocytes of hyperproliferative epithelia is not a result of the concomitant inflammation. Furthermore, we do not think it likely that up-regulation of S100A8 and S100A9 expression is a straightforward effect of activin signaling, because 1) S100A8 and S100A9 were not up-regulated in the almost normal back skin of the activin-overexpressing mice (Fig. 6), 2) S100A8 and S100A9 were induced in only some of the activin-overexpressing HaCaT cells, which represented a mostly K10-positive differentiated subpopulation (Fig. 9), and 3) we did not obtain evidence of a direct induction of the S100A8 gene in activin-treated HaCaT cells (data not shown). Rather, we observed an increase in S100A8 expression in confluent non-transfected or vector-transfected HaCaT cells, which undergo partial differentiation, as reflected by expression of K10 and other markers (49), in comparison to subconfluent cells.[3] This correlates well with previous observations that expression of S100A8 and S100A9 in various epithelial cell lines is linked to their potential to undergo terminal differentiation (28). Thus, we believe that the expression levels of S100A8 and S100A9 in keratinocytes may be linked in a more complex way to the balance between proliferation and differentiation that is altered during wound healing and psoriasis as well as in the activin-overexpressing mice and in cultured keratinocytes.

There are several findings that indicate a role for S100A8 and S100A9 in epithelial differentiation. First, the genes for human S100A8 and S100A9 are co-localized in a cluster, the human epidermal differentiation complex, which also contains

[3] I. S. Thorey, S. Durka, and S. Werner, unpublished information.

the genes for other S100 proteins, several cytokeratins, and epidermal differentiation markers such as profilaggrin and involucrin; it has been suggested that expression of these genes could be coordinately regulated (50–52). Second, in accordance with our observations in HaCaT cells, the S100A8/A9 heterodimer was shown *in vitro* as well as in intact epithelial cells to bind to keratin filaments in a calcium-dependent manner (25, 53), and there is evidence for its association with the epidermal cytoskeleton in inflammatory dermatoses (14). It is not yet known whether S100A8/A9 binding to keratins has any functional consequences. However, the glial-specific Ca^{2+}-binding proteins, S100A1 and S100B, are capable of inhibiting the polymerization of glial intermediate filaments by binding to the subunit glial fibrillary acidic protein, thereby regulating the state of assembly of glial intermediate filaments (54, 55). In a similar manner, S100A8/A9 may possibly play a role in cytoskeletal reconstruction processes, which occur in those HaCaT cells that have begun to express K10 and that likewise may occur in hyperproliferative keratinocytes during wound healing or skin disease progression.

The detailed molecular processes that lead to up-regulation of S100A8 and S100A9 in epithelia during hyperproliferative processes remain to be elucidated. However, several findings implicate retinoids as negative regulators and the pro-inflammatory and pro-proliferative transcription factor nuclear factor interleukin 6 as a positive upstream regulator of S100A8 expression (56–58). Repression of S100A8 may thus explain some of the therapeutic effects of retinoids in inflammatory as well as hyperproliferative skin diseases.

Acknowledgment—We thank Christiane Born-Berclaz for excellent technical assistance.

REFERENCES

1. Clark, A. F. (1996) *The Molecular and Cellular Biology of Wound Repair*, 2nd Ed, pp. 195–248, Plenum Press, New York
2. Martin, P. (1997) *Science* **276,** 75–81
3. Harrison, C. A., Raftery, M. J., Walsh, J., Alewood, P., Iismaa, S. E., Thliveris, S., and Geczy, C. L. (1999) *J. Biol. Chem.* **274,** 8561–8569
4. Gabrielsen, T., Dale, I., Brandtzaeg, P., Hoel, P. S., Fagerhol, M. K., Eeg Larsen, T., and Thune, P. O. (1986) *J. Am. Acad. Dermatol.* **15,** 173–199
5. Brandtzaeg, P., Dale, I., and Fagerhol, M. K. (1987) *Am. J. Clin. Pathol.* **87,** 700–707
6. Odink, K., Cerletti, N., Brüggen, J., Clerc, R. G., Tarcsay, L., Zwadlo, G., Gerhards, G., Schlegel, R., and Sorg, C. (1987) *Nature* **330,** 80–82
7. Zwadlo, G., Brüggen, J., Gerhards, G., Schlegel, R., and Sorg, C. (1988) *Clin. Exp. Immunol.* **72,** 510–515
8. Lagasse, E., and Clerk, R. G. (1988) *Mol. Cell. Biol.* **8,** 2402–2410
9. Hogg, N., Allen, C., and Edgeworth, J. (1989) *Eur. J. Immunol.* **19,** 1053–1061
10. Edgeworth, J., Gorman, M., Bennett, R., Freemont, P., and Hogg, N. (1991) *J. Biol. Chem.* **266,** 7706–7713
11. Lagasse, E., and Weissman, I. L. (1992) *Blood* **79,** 1907–1915
12. Wilkinson, M. M., Busuttil, A., Hayward, C., Brock, D. J. H., Dorin, J. R., and van Heyningen, V. (1988) *J. Cell Sci.* **91,** 221–230
13. Kelly, S. E., Jones, D. B., and Fleming, S. (1989) *J. Pathol.* **159,** 17–21
14. Kelly, S. E., Hunter, J. A. A., Jones, D. B., Clark, B. R., and Fleming, S. (1991) *Br. J. Dermatol.* **124,** 403–409
15. Madsen, P., Rasmussen, H. H., Leffers, H., Honore, B., Dejgaard, K., Olsen, E., Kiil, J., Walbum, E., Andersen, A. H., Basse, B., Lauridsen, J. B., Ratz, G. P., Celis, A., Vandekerckhove, J., and Celis, J. E. (1991) *J. Invest. Dermatol.* **97,** 701–712
16. Madsen, P., Rasmussen, H. H., Leffers, H., Honore, B., and Celis, J. E. (1992) *J. Invest. Dermatol.* **99,** 299–305
17. Roth, J., Sunderkötter, C., Goebeler, M., Gutwald, J., and Sorg, C. (1992) *Int. Arch. Allergy Immunol.* **98,** 140–145
18. Kunz, M., Roth, J., Sorg, C., and Kolde, G. (1992) *Arch. Dermatol. Res.* **284,** 386–390
19. Munz, B., Smola, H., Engelhardt, F., Bleuel, K., Brauchle, M., Lein, I., Evans, L. W., Huylebroeck, D., Balling, R., and Werner, S. (1999) *EMBO J.* **18,** 5205–5215
20. Chomczynski, P., and Sacchi, N. (1987) *Anal. Biochem.* **162,** 156–159
21. Werner, S., Weinberg, W., Liao, X., Peters, K. G., Blessing, M., Yuspa, S. H., Weiner, R. I., and Williams, L. T. (1993) *EMBO J.* **12,** 2635–2643
22. Wilkinson, D., Bailes, J., Champion, J., and McMahon, A. (1987) *Development* **99,** 493–500
23. Komminoth, P., Merk, F. B., Leav, I., Wolfe, H. J., and Roth, J. (1992) *Histochemistry* **98,** 217–228
24. Goebeler, M., Roth, J., Henseleit, U., Sunderkötter, C., and Sorg, C. (1993) *J. Leukocyte Biol.* **53,** 11–18
25. Roth, J., Burwinkel, F., van den Bos, C., Goebeler, M., Vollmer, E., and Sorg, C. (1993) *Blood* **82,** 1875–1883
26. Frosch, M., Strey, A., Vogl, T., Wulffraat, N. M., Kuis, W., Sunderkötter, C., Harms, E., Sorg, C., and Roth, J. (2000) *Arthritis Rheum.* **43,** 628–637
27. Bhardwaj, R., Zotz, C., Zwadlo-Klarwasser, G., Roth, J., Goebeler, M., Mahnke, K., Falk, M., Meinardus-Hager, G., and Sorg, C. (1992) *Eur. J. Immunol.* **22,** 1891–1897
28. Saintigny, G., Schmidt, R., Shroot, B., Lennart, J., Reichert, U., and Michel, S. (1992) *J. Invest. Dermatol.* **99,** 639–644
29. Werner, S., Breeden, M., Hübner, G., Greenhalgh, D. G., and Longaker, M. T. (1994) *J. Invest. Dermatol.* **103,** 469–473
30. Frank, S., Madlener, M., and Werner, S. (1996) *J. Biol. Chem.* **271,** 10188–10193
31. Hübner, G., Brauchle, M., Smola, H., Madlener, M., Fässler, R., and Werner, S. (1996) *Cytokine* **8,** 548–556
32. Hübner, G., Hu, Q., Smola, H., and Werner, S. (1996) *Dev. Biol.* **173,** 490–498
33. Dammeier, J., Beer, H. D., Brauchle, M., and Werner, S. (1998) *J. Biol. Chem.* **273,** 18185–18190
34. Munz, B., Wiedmann, M., Lochmüller, H., and Werner, S. (1999) *J. Biol. Chem.* **274,** 13305–13310
35. Munz, B., Frank, S., Hübner, G., Olsen, E., and Werner, S. (1997) *Biochem. J.* **326,** 579–585
36. Frank, S., Munz, B., and Werner, S. (1997) *Oncogene* **14,** 915–921
37. Steiling, H., Munz, B., Werner, S., and Brauchle, M. (1999) *Exp. Cell Res.* **247,** 484–494
38. Fässler, R., Sasaki, T., Timpl, R., Chu, M.-L., and Werner, S. (1996) *Exp. Cell Res.* **222,** 111–116
39. Dorin, J. R., Novak, M., Hill, R. E., Brock, D. J. H., Secher, D. S., and van Heyningen, V. (1987) *Nature* **326,** 614–617
40. Abe, M., Umehara, F., Kubota, R., Moritoyo, T., Izumo, S., and Osame, M. (1999) *J. Neurol.* **246,** 358–364
41. Rammes, A., Roth, J., Goebeler, M., Klempt, M., Hartmann, M., and Sorg, C. (1997) *J. Biol. Chem.* **272,** 9496–9502
42. Katz, A. B., and Taichman, L. B. (1999) *J. Invest. Dermatol.* **112,** 818–821
43. Steinbakk, M., Naess-Andresen, C. F., Lingaas, E., Dale, I., Brandtzaeg, P., and Fagerhol, M. K. (1990) *Lancet* **336,** 763–765
44. Sohnle, P., Collins-Lech, C., and Weissner, J. (1991) *J. Infect. Dis.* **163,** 187–192
45. Brandtzaeg, P., Gabrielsen, T., Dale, I., Müller, F., Steinbakk, M., and Fagerhol, M. K. (1995) *Adv. Exp. Med. Biol.* **371,** 201–206
46. Lackmann, M., Rajasekariah, P., Iismaa, S. E., Jones, G., Cornish, C. J., Hu, S., Simpson, R. J., Moritz, R. L., and Geczy, C. L. (1993) *J. Immunol.* **150,** 2981–2991
47. Passey, R. J., Williams, E., Lichanska, A. M., Wells, C., Hu, S., Geczy, C. L., Little, M. H., and Hume, D. A. (1999) *J. Immunol.* **163,** 2209–2216
48. Pröpper, C., Huang, X., Roth, J., Sorg, C., and Nacken, W. (1999) *J. Biol. Chem.* **274,** 183–188
49. Ryle, C. M., Breitkreutz, D., Stark, H.-J., Leigh, I. M., Steiner, P. M., Roop, D., and Fusenig, N. E. (1989) *Differentiation* **40,** 42–54
50. Mischke, D., Korge, B. P., Marenholz, I., Volz, A., and Ziegler, A. (1996) *J. Invest. Dermatol.* **106,** 989–992
51. Hardas, B. D., Zhao, X., Zhang, J., Longqing, X., Stoll, S., and Elder, J. T. (1996) *J. Invest. Dermatol.* **106,** 753–758
52. South, A. P., Cabral, A., Ives, J. H., James, C. H., Mirza, G., Marenholz, I., Mischke, D., Backendorf, C., Ragoussis, J., and Nizetic, D. (1999) *J. Invest. Dermatol.* **112,** 910–918
53. Goebeler, M., Roth, J., van den Bos, C., Ader, G., and Sorg, C. (1995) *Biochem. J.* **309,** 419–424
54. Bianchi, R., Giambanco, I., and Donato, R. (1993) *J. Biol. Chem.* **268,** 12669–12674
55. Garbuglia, M., Verzini, M., Rustandi, R., Osterloh, D., Weber, D. J., Gerke, V., and Donato, R. (1999) *Biochem. Biophys. Res. Commun.* **254,** 36–41
56. Klein, E. S., Pino, M. E., Johnson, A. T., Davies, P. J. A., Nagpal, S., Thacher, S. M., Krasinski, G., and Chandraratna, R. A. S. (1996) *J. Biol. Chem.* **271,** 22692–22696
57. Nagpal, S., Thacher, S. M., Patel, S., Friant, S., Malhotra, M., Shafer, J., Krasinski, G., Asano, A. T., Teng, M., Duvic, M., and Chandraratna, R. A. S. (1996) *Cell Growth Differ.* **7,** 1783–1791
58. DiSepio, D., Malhotra, M., Chandraratna, R. A. S., and Nagpal, S. (1997) *J. Biol. Chem.* **272,** 25555–25559